ISSN 2181-8622

Manufacturing technology problems

Scientific and Technical Journal Namangan Institute of Engineering and Technology

Volume 8
Issue 4
2023

1-Ilova

NamMTI ILMIY-TEXNIKA JURNALI

Tahrir hay’ati a’zolari:

Paxtani dastlabki ishlash, to’qimachilik va yengil sanoat

1. Axmadxodjayev X.T., t.f.d., prof. - NamMTI
2. Muradov R.M., t.f.d., prof. - NamMTI
3. Jumaniyozov Q., t.f.d., prof. - “Paxtasanoat ilmiy markazi” OAJ
4. Eshmatov A.B., t.f.d., prof. - Tojikiston Milliy Texnologiyalar Universiteti
5. Xoliqov Q., t.f.d., prof. - NamMTI
6. Ergashev J.S., t.f.d., dots - NamMTI
7. Obidov A.A., t.f.d., dots. - NamMTI

Kimyo va kimyoviy texnologiyalar

1. Namazov Sh.S., t.f.d., prof., akad. - O’zR FA UNKI
2. Botirov E.X., k.f.d., prof. - O’zR FA O’MKI
3. Akbarov H.I., k.f.d., prof. - O’zMU
4. Boymirzayev A., k.f.d., prof. - NamMTI
5. Nurmonov S.E., t.f.d., prof. - O’zMU
6. Salihanova D.S., t.f.d., prof. - O’zR FA UNKI
7. Kattayev N.T., k.f.d., prof. - O’zMU

Ta’limda ilg’or pedagogik texnologiyalar

1. Goncherenko I.I., f.m.f.d., prof. - BMTU, Belorussiya
2. Hüseyin Kamal, t.f.d., prof. - Ege Universiteti, Turkiya
3. Ergashev Sh.T., t.f.n., dots. - NamMQI
4. Musayev J.P., p.f.d., prof. - IRV
5. Xoshimova D., f.f.d., prof. - NamMTI
6. Maxkamov A.M., t.f.d. - NamMTI

Qishloq xo’jaligi mahsulotlarini yetishtirish, saqlash,qayta ishlash va oziq-ovqat texnologiyalari

1. Toshev A., t.f.d., prof., akad. - Janubiy Ural davlat universiteti, Rossiya
2. Banu Yucel., q.x.f.d., prof. - Ege Universiteti, Turkiya
3. Alimov U., t.f.d. - O’zR FA UNKI
4. Xudayberdiyev A.A., t.f.d., prof. - NamMTI
5. Sherquziyev D.Sh., t.f.d., prof. - NamMTI
6. Merganov A., q.x.f.d., prof. - NamMTI
7. Mamatov Sh., t.f.d., prof. - Webster Universiteti

Mexanika va mashinasozlik

1. Zaynobiddinov S., f.m.f.d., prof., akad. -ADU
2. Mardonov B., f.m.f.d., prof. - TTYSI
3. Usmanov P., f.m.f.d., dots. - NamMTI
4. Matkarimov P.J., t.f.d., prof. - NamMTI
5. Sharibayev N., f.m.f.d., prof. - NamMTI
6. Erkaboyev U.I., f.m.f.d., dots. - NamMTI
7. Musoyev S.S., t.f.n., prof. - BuxMTI

Iqtisodiyot

1. Maniki Tiagi, i.f.d. - KIET, Xindiston
2. Malcolm Ng Cher Herh., t.f.d. - INTI IUC, Malaysia
3. Soliyev A., i.f.d., prof. - NamMTI
4. Saidboyev Sh., i.f.d., prof. - NamMTI
5. Matkarimov K., i.f.n., prof. - NamMTI
6. Kadirova X.T., i.f.d., dots. - NamMTI
7. Bustonov M.M., i.f.d., dots. - NamMTI

Muharrirlar guruhi

S. Yusupov, O. Kazakov, B. Xolmirzayev, A. Mirzaev,
A. Tursunov, O. R. Qodirov (mas’ul muharrir)

MODELING THE PRODUCTION OF DIMETHYL ETHER FROM NATURAL GAS

SHUKUROV JASUR

Doctoral student of Samarkand State University named after Sharaf Rashidov
E-mail: shukjasni@gmail.com

Abstract. The study utilizes the Katalco-58 industrial catalyst from Johnson Matthey Catalysts, composed of 13 wt.% Cu/27 wt.% ZnO/60 wt.% Al_2O_3, in the dehydration of methanol to DME. The catalytic activity of the samples was studied in an apparatus that allows the process to be investigated under steady-state conditions with a high-pressure flow reactor. The phase composition of the samples before and after catalytic tests was determined using a Shimadzu XRD-6000 diffractometer with unfiltered CuKα radiation (λ=1.5418 Å). The porous structure and specific surface area of the samples were identified using the Tristar II (3020) Brunauer-Emmett-Teller method. The specific surface area was determined from nitrogen adsorption isotherms observed at -197°C. The pore volume was determined at a relative pressure of P/P0=0.99. The initial reaction mixture used was a combination of hydrogen and carbon monoxide supplied from cylinders and fed to the reactor. Samples were tested at pressures between 1-5 MPa and temperatures between 220-300°C, in steps of 20°C. Products were analyzed by chromatographic analysis on a "Crystal 5000.2" gas chromatograph. The water content was determined by the Karl Fischer method.

Keywords: synthesis gas, dimethyl ether(DME), methanol, catalyst, conversion.

Introduction. Using natural gas as an energy and chemical raw material offers the opportunity to reduce the consumption of conventional fuels and produce necessary products. Currently, in the industry, methane and its homologs are converted catalytically to produce hydrogen, synthesis gas, ammonia, methanol, liquid fuel, and other products [1]. The process of producing synthesis gas as a result of the conversion of light hydrocarbons is essential[2] as it offers the production of a variety of products based on simple CO and H_2 molecules [3].One of the most developed processes in the industry is converting natural gas to methanol [4]. As not all plants can adapt to producing new products, it is promising to produce new materials based on existing technologies. For example, the production of dimethyl ether (DME), an alternative to diesel fuel, can be promoted based on existing methanol production [5]. The study of the effect of external pressure showed that the yield of DME is a parabolic relationship, the maximum of which corresponds to 2 MPa. CO conversion increases with increasing pressure[6]. The main industrial process for producing dimethyl ether is the catalytic dehydration of methanol, conducted at high pressures and temperatures of 270-310°C. However, achieving high selectivity in this temperature range is challenging, as carbonaceous deposits can form. Therefore, an additional purification step is necessary to ensure the purity of DME. The obtained synthesis gas has a noticeable effect on the production quality of both methanol and dimethyl ether, making it crucial to efficiently design the synthesis gas production stage. For economic efficiency, carbonate anhydride is used in the methane bubble conversion reactor. In this way, the bubbly conversion of methane is implemented, which not only addresses the issue of using carbonate anhydride but also significantly increases the carbon oxide concentration in the synthesis gas and decreases the hydrogen concentration[7].

For this process, there are two classes of catalysts: low-temperature sulfocation types such as Amberlist-15, Dowex-50, Ky-1, Ky-2, and oxide catalysts (aluminum, zirconium oxides). The disadvantages of the sulfocation catalysts are their low thermal stability (operating temperature range 80-150°C). The shortcomings of oxide catalysts, for instance, γ-Al_2O_3, include their low catalytic activity at temperatures below 200°C. This leads to the possible formation of side products and the necessity of additional expenses for heating the reactor. To overcome the above disadvantages, the 13 wt.% Cu/27 wt.% ZnO/60 wt.% Al_2O_3 polyoxide catalyst is suggested, which allows the hydration reaction of methanol at a temperature range of 120-220°C. Based on literature data, a step-by-step mechanism for the dehydration reaction of methanol in γ-Al_2O_3 catalyst has been adopted.

Currently, the day by day decrease of oil reserves puts the task of searching for an alternative source of energy to replace oil before the scientists of the world. Such alternative sources are natural gas and biomass. To date, scientists of the world are interested in obtaining ethylene in one step by oxycondensation of methane, taking methanol and diethers from methane through synthesis gas and synthesizing lower molecular alkenes based on them, and at the same time using petroleum satellite gases effectively, that is, obtaining lower molecular unsaturated hydrocarbons based on them [8-22]. Synthesis of the above-mentioned processes and substances that act as semi-products in petrochemical and organic synthesis is one of the urgent issues for today.

Experimental part. In this study, the industrial catalyst Katalco-58 from Johnson Matthey Calalysts, with a composition of 13 wt.% CuO/27 wt.% ZnO/60 wt.%Al_2O_3, was used for the dehydration of methanol to DME. For the simplified step-by-step mechanism of this dehydration reaction, an appropriate kinetic model was derived using the Horii method. During the model derivation, the adsorption-desorption stages were assumed to be fast. Methanol was chosen as the main reactant; hence, the formation rates of water and dimethyl ether (DME) were calculated based on constant ratios. To study the activity of the selected catalysts in the methanol dehydration reaction, laboratory flow-catalytic devices with catalyst volumes of 2 mL, 10 mL, 22 mL, and 100 mL were constructed and assembled. Synthetic gas-derived methanol was used as feedstock. The composition of the synthesis gas(CO,H_2) was analyzed using both gas chromatography and a portable gas analyzer. The amounts of oxygen, nitrogen, carbon monoxide (CO), carbon dioxide(CO_2), and hydrogen in the synthesis gas were determined. In all experiments, the results of gas analysis in the gas analyzer and gas chromatography matched well. Methods for gas chromatographic analysis of synthesis gas conversion to methanol and methanol hydration products were developed. Separators for clearly distinguishing oxygen and hydrocarbons in the gas chromatograph were selected. High precision in analyzing methanol, dimethyl ether, and water at any concentration in the reaction products was noted.

The study of the catalysts' activity was carried out in a device allowing the process to be studied under continuous conditions with a high-pressure flow reactor. The initial reaction mixture consisted of hydrogen and carbon monoxide fed from cylinders and mixed before entering the reactor. The samples were tested under pressures of 1-5 MPa and temperature ranges of 220-300°C with a 20°C increment. The products were analyzed on a "Crystal 5000.2" gas chromatograph. The amount of water was determined according to the Karl Fischer method. The phase composition of the investigated samples was determined before and after catalytic tests using the Shimadzu XRD-6000 diffractometer with unfiltered CuK_α radiation (λ=1.5418 Å) through X-ray phase analysis. Phase composition analysis was performed using the PCPDFWIN database and the multi-network programs POWDER CELL 2.4 and PDF 4+. The porous structure and specific surface area of the samples were identified using the Tristar II (3020) Brunauer-

Emmett-Teller (BET) method. The specific surface area was determined from nitrogen adsorption isotherms observed at -197°C. The pore volume was determined at a relative pressure of P/P0=0.99. The surface morphology of the samples was studied using a high-resolution digital DFC280 R2 camera equipped with a Leica optical polarization microscope and an electron microscope VEGA II LMU based on the energy-dispersive microanalysis system INCA ENERGY 350. This was done to study the structure and composition of natural objects using scanning electron microscopy and X-ray spectral analysis. The primary electron beam energy was 20 kV. Differential thermal analysis (DTA) of the samples was carried out on a combined TGA-DSC analyzer Q-600 (TA Instruments, USA). The heating rate in the air atmosphere was 10 °C /min, and the standard was Al_2O_3. Temperature Programmed Desorption (TPD) analysis was performed on the Chemisorb 2750 chemisorption analyzer. The sample was desorbed in a flow of a 10 vol.% H_2+Ar mixture, heating at a linear rate of 10°C/min up to 600°C. CO TPD investigation was conducted in the Chemisorb 2750 chemisorption analyzer. To determine the acidic properties of the samples, an FTIP-8300 IR-spectrometer was used. The initial vacuumed sample's IR spectra were recorded after introducing CO, at liquid nitrogen temperature, in the 400-6000 cm^{-1} range with 4 cm^{-1} resolution and collecting 100-400 scanner descriptions.

The interaction character between reagents and the surface of catalysts was studied using the temperature programmed desorption method in a thermosorption device combined with mass spectrometric analysis (TPD-MS). The heating rate was set at 9°C/min, and the gas flow rate was 19 mL/min. Before the experiment, the sample was heated in a helium flow at a rate of 20°C/min up to the desorption temperature and then kept at this temperature for 1 hour. Adsorption was carried out at 100°C for 30 minutes. The composition of the products of thermal desorption from the catalyst surface was studied in the QMS 300 quadrupole mass spectrometer, which can detect gas mixture components at pressures from 10 mbar to 1 bar and concentrations as low as 1 ppm.

Experimental results and their discussion. In the industrial synthesis of methanol(CH_3OH), DME is produced as an intermediate product on a copper-zinc-aluminum catalyst. Two classes of catalysts were selected for the methanol dehydration reaction - acid catalysts with a polymer medium of moderate heat resistance and acid polyoxide catalysts made of oxides from groups III, IV, V of Dmitri Mendeleev's periodic table.

Modeling the kinetics of dimethyl ether synthesis from methanol: In the 13 wt.% CuO/27 wt.% ZnO/60 wt.% Al_2O_3 catalyst, the step-by-step mechanism of methanol dehydration reaction is. For this simplified step-by-step mechanism of methanol dehydration, the kinetic model corresponding to it can be obtained using the Horiuti method. In obtaining the model, the adsorption-desorption steps were assumed to be fast. Methanol was chosen as the primary substance, hence the formation rates of water and dimethyl ether (DME) were calculated based on constant ratios.The chemicals involved in the methanol dehydration reaction can be divided into two categories. The first category includes stable non-Bodenstein substances: methanol, dimethyl ether, and water. The second includes unstable Bodenstein substances: adsorbed methanol, dimethyl ether, water, and free active centers.We can formulate the main system of kinetic equations by distinguishing between Bodenstein and non-Bodenstein types. Rates of change in concentrations of non-Bodenstein (stable) substances:

$R^B_{CH_3OH} = -W_1$ (1)
$R^B_{CH_3OCH_3} = W_3$ (2)
$R^B_{H_2O} = W_4$ (3)

Rates of change in concentrations of Bodenstein (unstable) substances:

$R^B_{\Theta} = -W_1 + W_3 + W_4$ (4)
$R^B_{CH_3OH\Theta} = W_1 - 2W_2$ (5)
$R^B_{CH_3OCH_3\Theta} = W_2 - W_3$ (6)
$R^B_{H_2O\Theta} = W_2 - W_4$ (7)

Using Bodenstein's quasi-stationary approach, we get:

$R^B_{\Theta} + R^B_{CH_3OH\Theta} + R^B_{CH_3OCH_3\Theta} + R^B_{H_2O\Theta} = 0$ (8)
$X_{\Theta} + X_{CH_3OH\Theta} + X_{CH_3OCH_3\Theta} + X_{H_2O\Theta} = 1$ (9)

Expressing the rates of fast steps through the rates of slow steps (limiting rate):

From$R^B_{CH_3OH\Theta} = W_1 - 2W_2$, we get $W_1 = 2W_2$
From$R^B_{CH_3OCH_3\Theta} = W_2 - W_3$, we get $W_2 = W_3$
From$R^B_{H_2O} = W_2 - W_4$, we get $W_2 = W_4$

From the above, we deduce the kinetic model as:

$R^B_{CH_3OH\Theta} = -2W_2$ (10)
$R^B_{CH_3OCH_3\Theta} = W_2$ (11)
$R^B_{H_2O} = W_2$ (12)

Since the total matrix of reaction rates is of degree 1 in direction, we can have one primary component. We can choose methanol as the primary component and dimethyl ether and water as secondary components. Their concentrations can be expressed through invariant ratios:

$R^B_{CH_3OCH_3} = R^B_{H_2O} = -\frac{R^B_{CH_3OH}}{2}$ (13)

To calculate the rate of change of benzene, methanol, water, and dimethyl ether, it is necessary to use the equations (10)-(12).

$R^B_{CH_3OH} = -2W_2 = -2(W_{+2} - W_{+2}) = 2(k_{+2}X^2_{CH_3OH\Theta} - k_{-2}X_{CH_3OCH_3\Theta}X_{H_2O\Theta})$(14)

The concentration of unstable (intermediate) substances is expressed through the concentration of stable substances:

$X_{CH_3OH\Theta} = K_{(1)}X_{CH_3OH}X_{\Theta}$ (15)
$X_{CH_3OCH_3\Theta} = (K_{(3)})^{-1}X_{CH_3OCH_3}X_{\Theta}$ (16)
$X_{H_2O\Theta} = (K_{(4)})^{-1}X_{H_2O}X_{\Theta}$ (17)

Substituting the equations (15)-(17) into the invariant relationship $X_{\Theta} + X_{CH_3OH\Theta} + X_{CH_3OCH_3\Theta} + X_{H_2O\Theta} = 1$ we obtain:

$X_{\Theta} = \frac{1}{1+K_{(1)}X_{CH_3OH}+(K_{(3)})^{-1}X_{CH_3OCH_3}+(K_{(4)})^{-1}X_{H_2O}}$ (18)

$X_{CH_3OH\Theta} = \frac{K_{(1)}X_{CH_3OH}}{1+K_{(1)}X_{CH_3OH}+(K_{(3)})^{-1}X_{CH_3OCH_3}+(K_{(4)})^{-1}X_{H_2O}}$ (19)

$X_{CH_3OCH_3\Theta} = \frac{(K_{(3)})^{-1}X_{CH_3OCH_3}}{1+K_{(1)}X_{CH_3OH}+(K_{(3)})^{-1}X_{CH_3OCH_3}+(K_{(4)})^{-1}X_{H_2O}}$ (20)

$X_{H_2O\Theta} = \frac{(K_{(4)})^{-1}X_{H_2O}}{1+K_{(1)}X_{CH_3OH}+(K_{(3)})^{-1}X_{CH_3OCH_3}+(K_{(4)})^{-1}X_{H_2O}}$ (21)

$R^B_{CH_3OH} = \frac{-2k_{+2}(K_{(1)})^2X^2_{CH_3OH}+2k_{-2}(K_{(3)})^{-1}(K_{(4)})^{-1}X_{CH_3OH}X_{H_2O}}{(1+K_{(1)}X_{CH_3OH}+(K_{(3)})^{-1}X_{CH_3OCH_3}+(K_{(4)})^{-1}X_{H_2O})^2}$ (22)

The rate of change of methanol concentration is expressed through the concentration of stable substances, while the rate of change in the concentrations of water and dimethyl ether is calculated based on invariant ratios.

In conclusion, the kinetic model of the synthesis reaction of dimethyl ether(DME) can be represented as:

$$R^{B}_{CH_3OH} = \frac{-2k_{+2}(K_{(1)})^2\left(K^2_{CH_3OH}+\frac{P_{CH_3OCH_3}P_{H_2O}}{K_p}\right)}{(1+K_{(1)}X_{CH_3OH}+(K_{(3)})^{-1}X_{CH_3OCH_3}+(K_{(4)})^{-1}X_{H_2O})^2} \qquad (23)$$

where $K_p = \frac{P_{CH_3OCH_3}P_{H_2O}}{P^2_{CH_3OH}}$ -is the equilibrium constant of the dimethyl ether synthesis reaction,

$$K_{complex1} = 2k_{+2}(K_{(1)})^2,$$

$$K_p = K_{complex2} = 2k_{+2}(K_{(1)})^2/k_{-2}(K_{(3)})^{-1}(K_{(4)})^{-1}$$

are the cumulative kinetic constants (equilibrium constant of the DME synthesis reaction), and P - is the pressure in the reactor.

Evaluation of the kinetic experiments results and model constants of the methanol dehydration reaction: The experiments were carried out in various concentrations of methanol in raw materials, at a liquid flow rate of 0.5-12 hours^{-1}, and in a reaction zone temperature ranging from 90°C to 180°C. Generally, both types of catalysts showed similar activity at the same reaction temperature; additionally, above 160°C, the polymerizing catalyst rapidly lost its activity. The results of the first series of experiments in the laboratory apparatus are presented in Table 1. The data in Table 1 indicate that the first, second, and fourth stages of the process can be quickly calculated, and the methanol-dimethyl ether system is almost balanced. According to the experimental results, the parameters of the kinetic model were estimated using the linear least squares method.

The model's differential equations were solved using the fourth-order semi-implicit Runge-Kutta method. This method requires calculating the right side of the equation four times at each step. The general error of this method is of order 0(h^4).

The suitability of the model to the experiment was maximized using the Newton method and random sample search. The model predictions match the experimental data very well, with a discrepancy not exceeding 5%.

Table 1

Results of the first series of kinetic experiments on the activity study of the 13 wt.% CuO/27 wt.% ZnO/60 wt.%Al$_2$O$_3$ catalyst

Experimen t№	Methanol Molar Flow Rates, mol/hour	T, K	P, MPa	Methanol Conversion, %	
				Experimental	Calculated
1.	2.46	413	0.10	15.1	14.90
2.	2.46	423	0.10	32.2	31.22
3.	2.46	433	0.10	51.9	52.79
4.	2.46	443	0.10	73.5	73.78
5.	2.46	453	0.10	86.0	85.77
6.	4.18	463	0.17	90.5	90.26
7.	4.18	423	0.17	43.9	43.89
8.	4.18	433	0.17	64.5	64.36
9.	4.18	443	0.17	81.8	81.78
10.	4.18	453	0.17	89.4	89.57

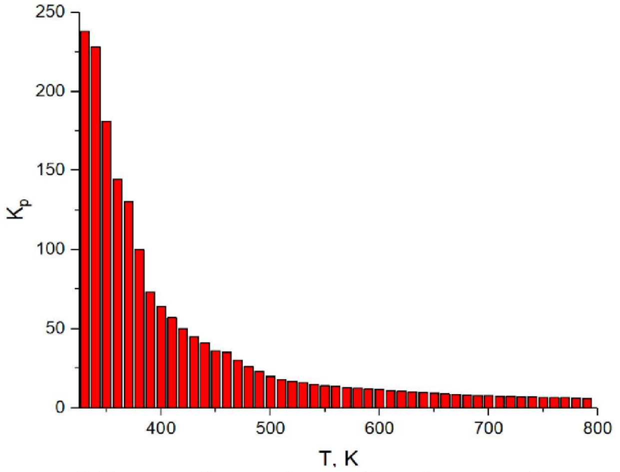

Figure 1. Dependence of the methanol synthesis reaction equilibrium constant on the reaction temperature

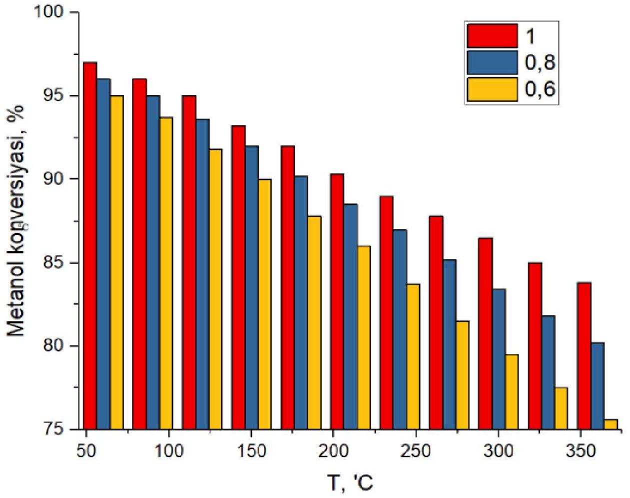

Figure 2. Dependence of the degree of methanol conversion on temperature at 1 atm pressure and initial mixtures with molar fractions of methanol being 0.6 (∆), 0.8 (*), 1.0 (□)

Modeling methanol dehydration reactions in a laboratory reactor. Results of modeling the dehydration reactions of methanol in a tubular flow reactor with an inner tube diameter of 2 cm, a reaction zone length of 31.8 cm, and a loaded catalyst volume V_{cat}= 0.1 L are presented in FIGUREures 3-6.

For the synthesis of DME from methanol, it is also necessary to study in detail the effect of water on the work of the catalyst, as water poisons all inorganic acid catalysts. However, sulfo-cationite catalysts, unlike poisoning by water, are regenerable. When water is desorbed from an inorganic catalyst (polyoxide compositions), it maintains its activity, which is an advantage over sulfo-cationite samples.

Between temperatures of 413-423 K, a low conversion rate of methanol was observed:

T=413 К, P=0,1 MPa, n^o_M=4.18 mol/hour
Methanol conversion rate – 9.35%

T=413 К, P=0,17 MPa, n^o_M=4.18 mol/hour
Methanol conversion rate– 21.39%
T=423 К, P=0,17 MPa, n^o_M=4.18 mol/hour
Methanol conversion rate– 42.96%

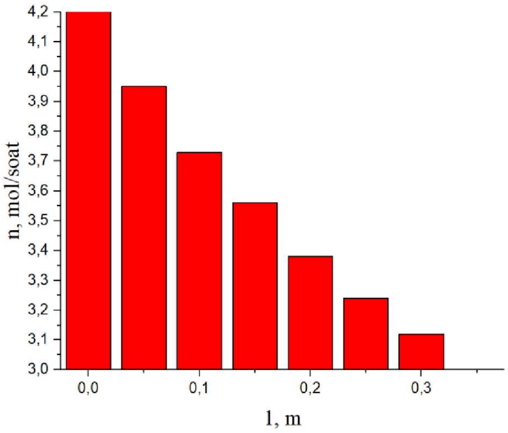

Figure 3. Change in methanol molar flow along the reactor length: T=423 К, P=0,2 MPa, n^o_M=4.18 mol/hour

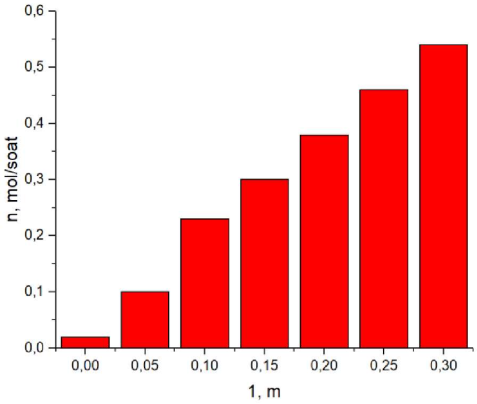

Figure 4. Change in DME molar flow along the reactor length: T=413 K, P=0.2 MPa, n^o_M=4.18 mol/hour. Methanol conversion 26.88%

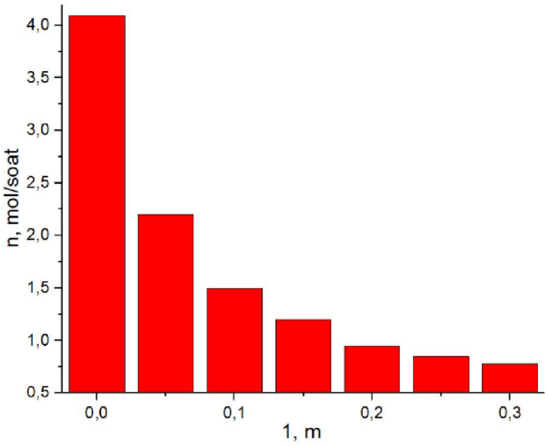

Figure 5. Variation of methanol molar flow along the reactor length: T=443 K, P=0.2 MPa, n^o_M=4.18 mol/hour, n^o_{DME}=0.2 mol/hour, n_{water}=0.2 mol/hour

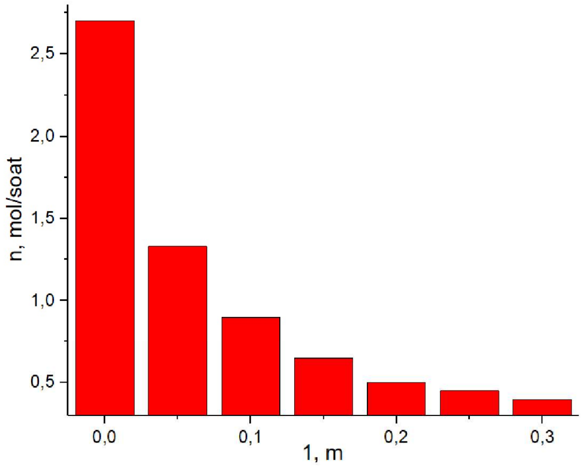

Figure 6. Variation of methanol molar flow along the reactor length: T=413 K, P=1.0 MPa, n^{o}_{M}=2.75 mol/hour. Methanol conversion 93.3 %

Long-term stability tests of the 13 wt.% CuO/27 wt.% ZnO/60 wt.%Al_2O_3 catalyst were conducted over 1000 hours of operation. Moreover, it was found that the catalyst almost did not lose its activity under the conditions of P=0.2 MPa and T = 181. In a 13 wt.% Cu/27 wt.% ZnO/60 wt.% Al_2O_3, methanol can be efficiently converted to dimethyl ether (DME) at a volumetric rate of 0.8 h^{-1}. At the end of the research phase dedicated to studying the chemical transformation process, we turn to the analysis of the catalyst particle and its behavior in the catalytic reactor. A quasi-homogeneous model was used as a particle model. Macrokinetic parameters of the model were calculated using known correlation equations and were further refined with experimental data. Efficiency factors for the catalyst granules were calculated accordingly. Apparently, the efficiency factor values for all substances are approximately 0.6.

The catalyst (a new high-silica zeolite catalyst 13 wt.% CuO/27 wt.% ZnO/60 wt.%Al_2O_3) is distinguished by its crystalline, porous structure. The new catalyst allows processing a wide range of raw hydrocarbons. As a result, high-octane additives (with an octane number of 90-91) can be obtained from gas condensate, and the propane(C_3)-butane(C_4) fraction is reprocessed into alkyl aromatic hydrocarbons.

During the experiment, catalyst tablets of sizes 3x3 mm and 6x4 mm of 13 wt.% CuO/27 wt.% ZnO/60 wt.%Al_2O_3 were used. Ignoring the impact of diffusion on similar-sized tablets for the catalytic process is not feasible. Therefore, the process was analyzed at the level of the catalyst particle. The particle model is as follows:

$$\frac{1}{R^2}\cdot\frac{d}{dR}\cdot\left(R^2 D_1(R)\frac{dc}{dR}\right)=K_S S(c-c_i)\ \frac{1}{r^2}\cdot\frac{d}{dr}\cdot\left(r^2 D_2(r)\frac{dc}{dr}\right)=R_i^B(c_i,r)$$
$$\frac{1}{R^2}\cdot\frac{d}{dR}\cdot\left(R^2\lambda_1(R)\frac{dc}{dR}\right)=\alpha_S S(T-T_i)\qquad \frac{1}{r^2}\cdot\frac{d}{dr}\cdot\left(r^2\lambda_2(r)\frac{dc}{dr}\right)=\sum_{u=1}^{p}\Delta H_u r^H(T_i,\vec{c}_i\ ) \quad (24)$$

Boundary conditions:

$$R=0\ \frac{dc}{dR}=0\,\frac{dT}{dR}=0 \quad R=R_3\ c(R_3)=c_{surf} \quad T(R_3)=T_{surf} \quad R=0\ \frac{dc}{dr}=0\,\frac{dT}{dr}=0 \ (25)$$
$$K_S S(c-c_i)=D\left.\frac{dc}{dr}\right|_{r=r\_\kappa p}\ r=r_{rp}\ \ \alpha_S S(T-T_i)=\lambda\bullet\left.\frac{\partial T}{\partial r}\right|_{r=r\_\kappa p}$$

Specific efficiency factor values for different reactants are: Methanol – 1.02, Dimethyl ether – 1.01, Ethylene – 0.99, Propylene – 0.98, Butylene – 0.97, Cyclohexane – 0.95, Methylcyclohexane – 0.91, Benzene – 0.93, Toluene, xylenes – 0.87, Trimethylbenzenes – 0.87, Tetramethylbenzenes – 0.86.

Based on the conducted kinetic studies and the analysis of the catalyst particle's performance, it was determined: For methanol dehydration reaction, a zeolite catalyst with the following characteristics is required

Si/Al ratio 75-200, Zeolite particle diameter1 μ, Zeolite-binder ratio– 0.6, Catalyst particle size, Diameter – 4 mm

Height – 2 mm.

DME synthesis catalytic reactor model: The device's scheme and description. The operation of catalytic drying is as follows figure 7 model of demethyl ether extraction device from synthesis gas. The system is cleansed with nitrogen, and operating pressure is generated by employing valves (1)-(6). The pressure is controlled by manometers (7)-(8) using" up to " (9) pressure regulator. Work safety is provided by an alarm device (10). Carbon (II) oxide and hydrogen are delivered to the reactor via two independent pipelines, pressure regulators from cylinders and dust filters in gas flow regulators. Hydrogen and carbon (II) oxide are then delivered into the catalytic reactor (15) through barrier-capable and reverse valves, where they are combined at the reactor entry and heated to the required temperature. The reactor block is made up of a reactor, an electric furnace, and a reverse valve system. The reactor is comprised of a stainless steel pipe with a 12 mm internal diameter. A one-zone electric furnace heats the reactor, allowing the temperature above the catalyst layer to be maintained with a 5^{0}C error. The reactor block is linked to a TXA controller chromalumel thermopara (0-1200^{0}C) thermometer (17), which is placed in the catalyst layer (16) and controls the four-channel temperature as specified. A glass fiber catalyst passage grating is positioned at the bottom of the reactor, where the catalyst is located. The catalyst layer is 4.4 cm tall, and the temperature ranges from 200 to 300 °C.The temperature of the oven and the Steamer are both adjusted simultaneously.

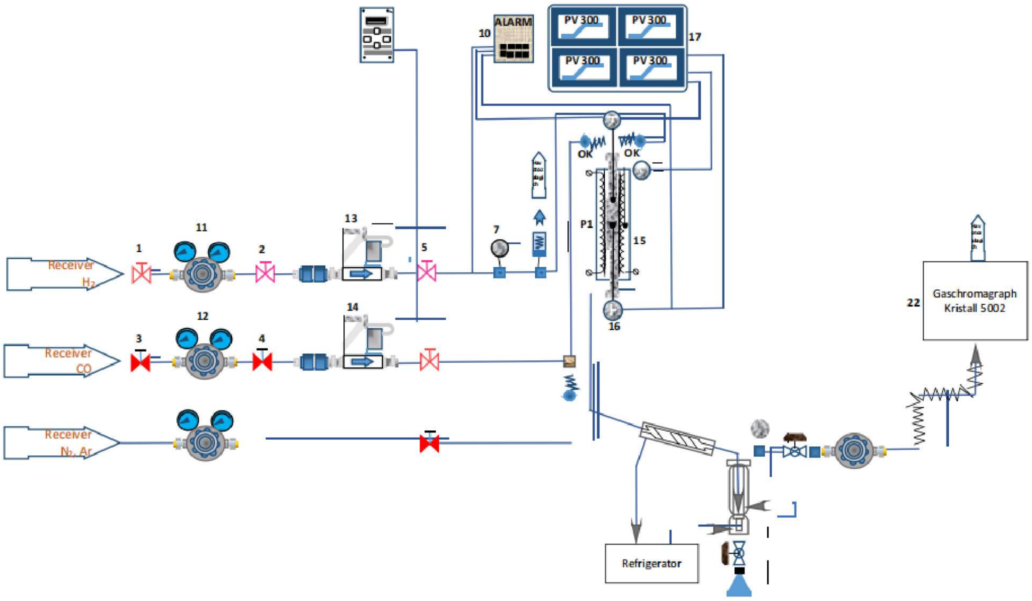

Figure 7. Model of demethyl ether extraction device from synthesis gas

In order to remove the water, methanol and hydrocarbons (dimethyl ether, CO, H_2, CO_2, CH_4, methanol vapor) formed after the reaction in the reactor, the gas mixture of the products is removed from the system with a one-time cooler (18) and circulating water at room temperature. passes through the separation device in the high-pressure separator (19) and, after separating the products in the high-pressure separator, is lowered into the condensate receiver (21) through the condensate adjustment valve (20). Gas products leave the high-pressure separator through the side nozzle, screw, back return pressure reducer (9) with the help of a suction fan, through the analytical control system (22).

$$u\frac{\partial \vec{c}}{\partial l} + D\left[\frac{\partial^2 c}{\partial r^2} + \frac{1}{r}\frac{\partial c}{\partial r}\right] \pm [K]S_H(\vec{c} - \vec{c}_{surf}) = 0$$

$$uc_p\rho\frac{\partial \vec{T}}{\partial l} + \lambda\left[\frac{\partial^2 T}{\partial r^2} + \frac{1}{r}\frac{\partial T}{\partial r}\right] \pm [\alpha]S_H(T - T_{surf}) = 0 \qquad (25)$$

$$[\eta]R^b\,(\vec{c}_{surf}, T_{surf}) = [K]S_H(\vec{c} - \vec{c}_{surf})$$

$$\sum_{u=1}^{p} \Delta H_u \vec{\eta}_u r_u\,(\vec{c}_{surf}, T_{surf}) = [\alpha]S_H(T - T_{surf})$$

Boundary conditions:

l=0 $\vec{c}(0,r) = \vec{c}_{inlet}(r)$ $T(0,r) = T_{inlet}(r)$

r=0 $\frac{\partial \vec{c}}{\partial r} = 0$ $\frac{\partial T}{\partial r} = 0$

r=R $\frac{\partial \vec{c}}{\partial r} = 0$ $\lambda \bullet \frac{\partial T}{\partial r}\Big|_{r=r\_кр} = (T - T_{ambient})$

where: λ – thermal conductivity of the stream; D – diffusion (backflow) coefficient of the flow; [K] – mass transfer coefficients for reactors; [α] – mass transfer coefficient from the particle to the flow; C_p– heat capacity of the mixture; ρ – density of the mixture; [η] – efficiency factor matrix for reactants; $[\vec{\eta}]$ – direction-specific final reaction efficiency factor matrix; ΔH_u –heat effect of the u-reaction; S – gas-solid phase separation interface; $\vec{c}$–reactant concentration in the gaseous phase; $\vec{c}_{surf}$ –reactant concentration on the catalyst surface.

Conclusion. The selectivity and yield of methanol conversion products are notably evident in catalysts composed of 13 wt.% CuO/27 wt.% ZnO/60 wt.% Al_2O_3.

From the results of testing various model samples, we selected the composition of the catalysts and the conditions of the process, achieving both high efficiency and integral selectivity for the targeted products.

When methanol undergoes the conversion process with carbon monoxide without the presence of an inert gas, the reactor's productivity remains largely unchanged.

It's possible to separate the products from the altered gas by cooling the converted gas and condensing them. The mixture of methyl formate, formaldehyde, and dimethyl ether derived from methanol can be isolated from water using distillation, given the significant differences in the boiling points of these components.

A rise in temperature results in a marginal decrease in methanol conversion. This observation aligns with experimental data, indicating that methanol conversion trends towards an equilibrium state.

References

1. P. DjinoVić, F.Schüth, Energy Carriers Made from Hydrogen, Electrochemical Energy Storage for Renewable Sources and Grid Balancing, ElseVier. (2015) 183–199.

2. Bukhorov A. Q., Aslanov S. C., Fayzullaev N. I. Direct extraction of dimethyl ether from synthesis gas //AIP Conference Proceedings. – AIP Publishing LLC, 2022. – T. 2432. – №. 1. – C. 050013.

3. E. V. Pisarenko, V. N. Pisarenko. "Modeling the low-temperature synthesis of dimethyl ether from methanol", Theoretical Foundations of Chemical Engineering, 2014

4. Shukurov J., Fayzullaev N. (2023). Catalyst selection and technology for obtaining dimethyl ether. *Universum: химия и биология*, (6-2 (108)), 57-61.

5. Bukhorov A. Q., Aslanov S. C., Fayzullaev N. I. Kinetic laws of dimethyl ether synthesis in synthesis gas //AIP Conference Proceedings. – AIP Publishing LLC, 2022. – T. 2432. – №. 1. – C. 050012.

6. Shukurov J., Fayzullaev N. Kinetic laws of dimethyl ether synthesis reaction //E3S Web of Conferences. – EDP Sciences, 2023. – T. 389. – C. 01037.

7. Musulmonov N. X., Fayzullaev N. I. Textural characteristics of zinc acetate catalyst //AIP Conference Proceedings. – AIP Publishing LLC, 2022. – T. 2432. – №. 1. – C. 050015.

8. Bukhorov A. Q., Aslanov S. C., Fayzullaev N. I. Catalyst deactivation in synthesis of olefins below methanol //AIP Conference Proceedings. – AIP Publishing LLC, 2022. – T. 2432. – №. 1. – C. 050010

9. F N Temirov, J Kh Khamroyev, N I Fayzullayev, G Sh Haydarov and M Kh Jalilov. Hydrothermal synthesis of zeolite HSZ-30 based on kaolin //IOP Conference Series: Earth and Environmental Science. – IOP Publishing, 2021. – T. 839. – №. 4. – C. 042099.

10. Khamroyev, J.K., Akmalaiuly, K., Fayzullayev, N. Mechanical activation of navbahorsk bentonite and its textural and adsorption characteristics//News of the National Academy of Sciences of the Republic of Kazakhstan, Series of Geology and Technical Sciences, 2022, 1(451), стр. 167–174.

11. Buronov F., Fayzullayev N. Synthesis and application of high silicon zeolites from natural sources //AIP Conference Proceedings. – AIP Publishing LLC, 2022. – T. 2432. – №. 1. – C. 050004.

12. Fayzullaev, N.I, Bobomurodova, S.Y, Xolmuminova, D.A Physico-chemical and texture characteristics of Zn-Zr/VKTS catalyst//Journal of Critical Reviews, 2020, 7(7), стр. 917–920

13. Fajzullaev, N.I., Fajzullaev, O.O. Kinetic regularities in reaction of the oxidizing condensation of methane on applied oxide catalysts//Khimicheskaya Promyshlennost', 2004, (4), стр. 204–207

14. Sarimsakova, N.S., Fayzullaev, N.I., Musulmonov, N.X., Atamirzayeva, S.T., Ibodullayeva, M.N. Kinetics and mechanism of reaction for producing ethyl acetate from acetic acid//International Journal of Control and Automation, 2020, 13(2), стр. 373–382.

15. Omanov, B.S., Fayzullaev, N.I., Musulmonov, N.K., Xatamova, M.S., Asrorov, D.A.Optimization of vinyl acetate synthesis process//International Journal of Control and Automation, 2020, 13(1), стр. 231–238

16. Omanov, B.S., Fayzullaev, N.I., Xatamova, M.S. Vinyl acetate production technology//International Journal of Advanced Science and Technology, 2020, 29(3), стр. 4923–4930

17. Xolmirzayeva H. N., Fayzullayev N. I. Obtaining Nanocarbon from Local Raw Materials and Studying Its Textural and Sorption Properties //International Journal of Engineering Trends and Technology, 2022 Volume 70 Issue 2, 163-171. ISSN: 2231 – 5381 /doi:10.14445/22315381/IJETT-V70I2P219

18. Aslanov, S.C., Buxorov, A.Q., Fayzullayev, N.I. Catalytic synthesis of C_2-C_4-alkenes from dimethyl ether// International Journal of Engineering Trends and Technology, 2021, 69(4), стр. 67–75

19. Jasur Shukurov, Normurot Fayzullaev. (2023). Kinetic Laws of the Reaction of Dimethyl Ether Synthesis from Synthesis-Gas, *International Journal of Materials and Chemistry*, (13)1,5-10.

20. S. H. Park, C. S. Lee, Applicability of dimethyl ether (DME) in a compression ignition engine as an alternatiVe fuel, Energy ConVersion and Management. 86 (2014) 848–863.

21. Shukurov, J., Fayzullaev, N., Turayev, B. & Kungratov K. (2023).Technology of extraction of dimethyl ether from methanol. *Universum: технические науки*, 6(111), 46-49.

22. Bukhorov A. Q., Aslanov S. C., Fayzullaev N. I. Conversion of dimethyl ether to lower olefines //AIP Conference Proceedings. – AIP Publishing LLC, 2022. – Т. 2432. – №. 1. – С. 050011.

UDC 661.152.5

STUDY OF INTERACTION OF COMPONENTS IN $ZnSO_4$ – NH_4H_2PO4 – H_2O SYSTEM

MAKHKAMOVA DILNOZA

Doctoral student Namangan Institute of Engineering and Technology
E-mail: dilnozamaxkamova_7007@mail.ru, phone.: (+99897) 120 08-07

TURAEV ZOKIRJON

Professor of Namangan Institute of Engineering and Construction
E-mail: T-Zokirjon@umail.uz, phone.: (+99893) 403 40-04

DEDABOYEVA MAHLIYO

Assistant of Namangan Institute of Engineering and Construction
E-mail.: mahliyo.dedaboeva@gmail.com, phone.: (+99893) 800 87-25

Abstract:

Objective. To theoretically substantiate the interaction of zinc sulfate with monoammonium phosphate, an isomolar series was used, based on the ratio of the components $ZnSO_4$ and $NH_4H_2PO_4$.

Methods. The physicochemical properties of diluted solutions were studied by the isomolar series method to justify the interaction between zinc sulfate and monoammonium phosphate. Based on the ratio of components in the $ZnSO_4$ and $NH_4H_2PO_4$ system, pH value, density, refractive index, viscosity and crystallization temperature of the mixture of 0,01 M solutions were measured.

Results. According to the results of the physicochemical characteristics of diluted solutions in the [$ZnSO_4$(0.01M)]:[$NH_4H_2PO_4$(0.01M)] system, i.e., the pH environment, density, viscosity, refractive index and crystallization temperature values, one deviation corresponding to the presence networks of the initial components is observed. Based on the results of the diagram, it is expressed in the ratio [$ZnSO_4$(0.01M)]:[$NH_4H_2PO_4$(0.01M)]=4:6.

Conclusion. From the obtained results, it can be concluded that changes in the physicochemical properties of solutions occur even at the above amount of zinc sulfate and monoammonium phosphate with the composition ratio [$ZnSO_4$(0.01M)]:[$NH_4H_2PO_4$(0.01M)]=4:6. This shows that regardless of the initial concentration of zinc sulfate, when a small amount of monoammonium phosphate is added, a change in the composition of the solution occurs.

Keywords: zinc sulfate, monoammonium phosphate, Ostromyslensky-Job isomolar series method, pH value, density, viscosity, refractive index, crystallization temperature.

CONTENTS

PRIMARY PROCESSING OF COTTON, TEXTILE AND LIGHT INDUSTRY

GROWING, STORAGE, PROCESSING AND AGRICULTURAL PRODUCTS AND FOOD TECHNOLOGIES

CHEMICAL TECHNOLOGIES

MECHANICS AND ENGINEERING

ADVANCED PEDAGOGICAL TECHNOLOGIES IN EDUCATION

ECONOMICAL SCIENCES